# Nuclear Factor E2-Related Factor 2-Dependent Myocardiac Cytoprotection Against Oxidative and Electrophilic Stress

By: Hong Zhu, Zhenquan Jia, Bhaba R. Misra, Li Zhang, Zhuoxiao Cao, Masayuki Yamamoto, Michael A. Trush, Hara P. Misra, Yunbo Li

Zhu H, Jia Z, Misra BR, Zhang L, Cao Z, Yamamoto M, Trush MA, Misra HP, Li Y. 2008. Nuclear factor E2-related factor 2-dependent myocardiac cytoprotection against oxidative and electrophilic stress. *Cardiovascular Toxicology* 8(2):71-85.

**The final publication is available at Springer via http://dx.doi.org/10.1007/s12012-008-9016-0**



## Abstract:

Nuclear factor E2-related factor 2 (Nrf2) is a critical regulator of cytoprotective gene expression. However, the role of this transcription factor in myocardiac cytoprotection against oxidative and electrophilic stress remains unknown. This study was undertaken to investigate if Nrf2 signaling could control the constitutive and inducible expression of antioxidants and phase 2 enzymes in primary cardiomyocytes as well as the susceptibility of these cells to oxidative and electrophilic injury. The basal expression of a series of antioxidants and phase 2 enzymes was significantly lower in cardiomyocytes from $Nrf2^{-/-}$ mice than those from wild-type littermates. Incubation of wild-type cardiomyocytes with 3*H*-1,2-dithiole-3-thione (D3T) led to significant induction of various antioxidants and phase 2 enzymes, including catalase, glutathione, glutathione peroxidase (GPx), glutathione reductase, glutathione S-transferase, NAD(P)H:quinone oxidoreductase 1, and heme oxygenase-1. The inducibility of the above cellular defenses except GPx by D3T was abolished in $Nrf2^{-/-}$ cardiomyocytes. As compared to wild-type cells, $Nrf2^{-/-}$ cardiomyocytes were much more susceptible to cell injury induced by $H_2O_2$, peroxynitrite, and 4-hydroxy-2-nonenal. Treatment of wild-type cardiomyocytes with D3T, which upregulated the cellular defenses, resulted in increased resistance to the above oxidant- and electrophile-induced cell injury, whereas D3T treatment of $Nrf2^{-/-}$ cardiomyocytes provided no cytoprotection. This study demonstrates that Nrf2 is an important factor in controlling both constitutive and inducible expression of a wide spectrum of antioxidants and phase 2 enzymes in cardiomyocytes and is responsible for protecting these cells against oxidative and electrophilic stress. These findings also implicate Nrf2 as an important signaling molecule for myocardiac cytoprotection.

## Abbreviations

***ARE***: Antioxidant response element
***CDNB***: 1-chloro-2,4-dinitrobenzene
***D3T***: 3*H*-1,2-dithiole-3-thione
***DCIP***: 2,6-dichloroindophenol
***FBS***: Fetal bovine serum
***γGCL***: γ-Glutamylcysteine ligase
***GCLC***: γ-Glutamylcysteine ligase catalytic subunit
***GPx***: Glutathione peroxidase
***GR***: Glutathione reductase
***GSH***: Reduced glutathione
***GSSG***: Oxidized form of glutathione
***GST***: Glutathione S-transferase
***HNE***: 4-hydroxy-2-nonenal
***HO-1***: Heme oxygenasse-1
***MTT***: 3-[4,5-dimethylthiazol-2-yl]-2,5-diphenyltetrazolium bromide
***NQO1***: NAD(P)H:quinone oxidoreductase 1
***Nrf2*** :Nuclear factor E2-related factor 2
***PBS***: Phosphate buffered saline
***SIN-1***: 3-morpholinosydnonimine
***RT-PCR***: Reverse transcriptase-polymerase chain reaction
***SOD***: Superoxide dismutase

**Keywords:** Nrf2 | Cardiomyocytes | Antioxidants | Phase 2 enzymes | Oxidative stress | Electrophilic

**Article:**

## Introduction

It is increasingly recognized that oxidative and electrophilic stress are important mechanisms underlying various forms of cardiovascular diseases, including atherosclerosis, myocardial ischemia-reperfusion injury, chronic heart failure, as well as drug-induced cardiomyopathy [*1–4*]. As such, exogenous compounds with antioxidative properties are extensively applied to the intervention of cardiovascular injury [*5*, *6*]. However, the use of exogenous antioxidants, including vitamin E, in the intervention of human cardiac disorders has produced disappointing results, which might be related to the limited bioavailability and effectiveness in scavenging oxidative and electrophilic species, as well as other untoward effects (e.g., prooxidative properties) associated with these antioxidant compounds [*7–10*]. Another strategy for protecting against oxidative and electrophilic cardiac cell degeneration may be via chemically mediated upregulation of a series of endogenous antioxidants and phase 2 enzymes in cardiomyocytes. Such a strategy relies on a better understanding of both the constitutive and inducible expression of various cardiac cellular antioxidants and phase 2 enzymes as well as the underlying signaling mechanisms.

Recently, the nuclear factor E2-related factor 2 (Nrf2) is found to be an indispensable transcription factor that binds to the antioxidant response element (ARE) in the promoter region of a number of cytoprotective genes [*11*, *12*]. However, studies on the expression of a series of antioxidants and phase 2 enzymes as well as their molecular regulation by Nrf2 signaling in primary cardiomyocytes are lacking. In the present study, using neonatal cardiomyocytes from Nrf2-null ($Nrf2^{-/-}$) mice and wild-type ($Nrf2^{+/+}$) littermates, we have investigated the regulatory role of Nrf2 in constitutive expression as well as inducibility by the chemoprotectant, 3*H*-1,2-dithiole-3-thione (D3T) of various antioxidants and phase 2 enzymes, including superoxide dismutase (SOD), catalase, reduced glutathione (GSH), glutathione reductase (GR), glutathione peroxidase (GPx), glutathione S-transferase (GST), NAD(P)H:quinone oxidoreductase 1 (NQO1), and heme oxygenase (HO). This study for the first time has comprehensively characterized a series of key antioxidants and phase 2 enzymes in primary cardiomyocytes, and demonstrated a crucial role for Nrf2 signaling in regulating both the constitutive and D3T-inducible expression of the antioxidative and phase 2 defenses, as well as in determining the susceptibility of these cardiomyocytes to cell injury elicited by oxidants and electrophilic species. The findings of this study thus demonstrate Nrf2 signaling as an important pathway for myocardiac cytoprotection against oxidative and electrophilic stress.

## Methods

### Chemicals and Materials

D3T (99.8% purity) was the gift from Dr. Mary Tanga at SRI International (Menlo Park, CA) and Dr. Linda Brady at National Institute of Mental Health (Bethesda, MD). Dulbecco's modified Eagle's medium (DMEM), penicillin, streptomycin, fetal bovine serum (FBS), and Dulbecco's phosphate buffered saline (PBS) were purchased from Gibco-Invitrogen (Carlsbad, CA). Anti-γ-glutamylcysteine ligase (γGCL) antibody was obtained from Lab Vision (Fremont, CA). Anti-GR antibody was obtained from Abcam (Cambridge, MA). Anti-GST-A, -M, and -P antibodies were purchased from Alpha Diagnostic (San Antonio, TX). Anti-NQO1 and β-actin antibodies were provided by Santa Cruz Biotech (Santa Cruz, CA). All other chemicals and agents were purchased from Sigma Chemical (St. Louis, MO).

### Animals and Genotyping

Breeding pairs of $Nrf2^{+/-}$ (ICR/Sv129) mice were initially obtained from a colony at Tsukuba University and maintained in the animal facility at Virginia Tech. $Nrf2^{+/+}$ and $Nrf2^{-/-}$ mice were generated following the breeding procedures described previously ([*13*]. Purina laboratory animal chow and water were available ad libitum. Genotypes ($Nrf2^{+/+}$, $Nrf2^{-/-}$, and $Nrf2^{+/-}$) of the animals were determined by polymerase chain reaction (PCR) amplification of genomic DNA from tails as described before [*13*]. All the animal procedures were approved by the Virginia Tech Institutional Animal Care and Use Committee.

### Primary Cardiomyocyte Culture

Neonatal mice at the age of 1–3 days were euthanized via cervical dislocation. The hearts were removed aseptically, trimmed of atria and connective tissue, and rinsed extensively with ice-cold PBS. The cardiomyocytes were isolated using a Neomyts isolation system for mouse cardiomyocytes (Cellutron Life Technology, Baltimore, MD) according to the manufacturer's instruction. Briefly, the cardiac cells were dissociated from intact ventricles upon incubation in a tissue digestion solution at 37°C with continuous stirring. The cells released were collected by centrifugation at 500*g* for 1 min. The resulting cell pellets were resuspended in culture medium and filtered using a cell strainer of 100 μm size (BD Falcon, Redford, MA). After filtration, the cells were cultured in DMEM supplemented with 10% FBS, 50 U/ml penicillin, and 50 μg/ml streptomycin in tissue culture flasks at 37°C for 2 h to remove the residual cardiac fibroblasts. The cardiomyocytes in suspension were transferred into tissue culture flasks coated with SureCoat (Cellutron), and continuously cultured in DEME supplemented with 10% FBS, 50 U/ml penicillin, and 50 μg/ml streptomycin at 37°C in a humidified atmosphere of 5% $CO_2$. The cells were fed every 3 days, and used for experiments within 10 days after isolation. The purity of cardiomyocytes in culture was above 95%, as determined by incubation with a monoclonal anti-α-cardiac muscle actinin antibody, followed by staining with a mouse ExtraAvidin peroxidase staining kit (Sigma Chemical). For experiments, D3T dissolved in dimethyl sulfoxide (DMSO) was added to cell cultures with a final DMSO concentration of 0.1% (v/v). Control groups received equal amounts of DMSO.

### Preparation of Cell Extract

Cardiomyocytes were collected and resuspended in ice-cold 50 mM potassium phosphate buffer, pH 7.4, containing 2 mM EDTA and 0.1% Triton X-100. The cells were sonicated, followed by centrifugation at 13,000*g* for 10 min at 4°C. The supernatants were collected and the protein concentrations were measured using a Bio-Rad protein assay kit (Hercules, CA) with bovine serum albumin as the standard.

### Assay for SOD Activity

The SOD activity was measured according to the method of Spitz and Oberley [*14*] with slight modifications, as described before [*13*]. This assay is based on the inhibition of the superoxide-mediated reduction of nitroblue tetrazolium to formazan by SOD. The cellular SOD activity was calculated using a concurrently run SOD (Sigma Chemical) standard curve, and expressed as units per mg of cellular protein.

### Assay for Catalase Activity

The catalase activity was measured using the method described by Aebi [*15*]. In brief, to a quartz cuvette, 0.41 ml of 50 mM potassium phosphate buffer (pH 7.0) and 10 μl of sample were added. The reaction was initiated by adding 0.18 ml of 30 mM $H_2O_2$ (Sigma Chemical). The decomposition of $H_2O_2$ was monitored at 240 nm, 25°C for 2 min. The cellular catalase activity was expressed as μmol of $H_2O_2$ consumed per min per mg of cellular protein.

## Assay for GSH Content

The GSH content was measured by the *o*-phthalaldehyde-based fluorescence assay, which is specific for the determination of GSH at pH 8.0 [*13*]. Briefly, 10 µl of the sample was incubated with 12.5 µl of 25% metaphosphoric acid, and 37 µl of 0.1 M sodium phosphate buffer containing 5 mM EDTA, pH 8.0 at 4°C for 10 min. The samples were cleared of precipitated protein by centrifugation at 13,000*g* for 5 min at 4°C. The resulting supernatant (10 µl) was incubated with 0.1 ml of *o*-phthalaldehyde solution (0.1% in methanol) and 1.89 ml of the above phosphate buffer for 15 min at room temperature. Fluorescence intensity was then measured at an excitation wavelength of 350 nm and an emission wavelength of 420 nm using a Perkin-Elmer LS50B fluorometer. The cellular GSH content was calculated using a GSH (Sigma Chemical) standard curve, and expressed as nmol of GSH per mg of cellular protein.

## Assay for GR Activity

The GR activity assay is based on the NADPH consumption coupled with the reduction of oxidized form of glutathione (GSSG) to GSH by GR, as described previously [*13*]. The cellular GR activity was calculated using the extinction coefficient of 6.22 $mM^{-1}$ $cm^{-1}$, and expressed as nmol of NADPH consumed per min per mg of cellular protein.

## Assay for GPx Activity

The GPx activity was measured by the method of Flohe and Gunzler [*16*], which is based on the formation of GSSG from GPx-catalyzed oxidation of GSH by $H_2O_2$, coupled with NADPH consumption in the presence of exogenously added GR. The cellular GPx activity was calculated using the extinction coefficient of 6.22 $mM^{-1}$ $cm^{-1}$, and expressed as nmol of NADPH consumed per min per mg of cellular protein.

## Assay for GST Activity

The GST activity was measured according to the procedures described by Habig et al. [*17*], using 1-chloro-2,4-dinitrobenzene (CDNB) as a substrate. The cellular GST activity was calculated using the extinction coefficient of 9.6 $mM^{-1}$ $cm^{-1}$, and expressed as nmol of CDNB-GSH conjugate formed per min per mg of cellular protein.

## Assay for NQO1 Activity

The NQO1 activity was determined using dichloroindophenol (DCIP) as the two-electron acceptor, as described before [*13*]. The dicumarol-inhibitable cellular NQO1 activity was calculated using the extinction coefficient of 21.0 $mM^{-1}$ $cm^{-1}$, and expressed as nmol of DCIP reduced per min per mg of cellular protein.

## Assay for HO Activity

The HO activity was measured according to the procedures described by Naughton et al. [*18*] with slight modifications. Briefly, the harvested cells were resuspended in 100 mM potassium phosphate buffer, pH 7.4, containing 2 mM $MgCl_2$, and subjected to three cycles of freeze-thawing and finally sonicated on ice before centrifugation at 18,000*g* for 10 min at 4°C. As much as 100 µl (200 µg protein) of the supernatant was added to 200 µl of reaction mix containing 0.5 mM NADPH, 2 mM glucose-6-phosphate, 1 U/ml glucose-6-phosphate dehydrogenase, 0.2 mM hemin, and 1 mg/ml rat liver cytosol (as a source of biliverdin reductase) in 100 mM potassium phosphate buffer, pH 7.4, containing 2 mM $MgCl_2$. The reaction was conducted for 1 h at 37°C in the dark and terminated by addition of 300 µl chloroform. The extracted bilirubin was measured by the difference in absorbance between 464 nm and 530 nm (extinction coefficient = 40 $mM^{-1}$ $cm^{-1}$). The cellular HO activity was expressed as pmol of bilirubin formed per h per mg of cellular protein.

Reverse Transcriptase-Polymerase Chain Reaction (RT-PCR) Analysis of mRNA Levels

Total RNA from cardiomyocytes was extracted using Trizol reagent (Invitrogen, Carlsbad, CA). cDNA synthesis and subsequent PCR reaction were performed using Superscript II One-Step system (Invitrogen), as described before [*13*]. The sequences for the PCR primers are shown in Table 1. PCR products were separated by 1% agarose gel electrophoresis. Gels were stained with ethidium bromide and analyzed under ultraviolet light using an Alpha Innotech Imaging system (San Leandro, CA). Various amounts of total RNA were used for each of the antioxidative and phase 2 genes to demonstrate a linear amplification of the specific mRNA. The quantitative capacity of RT-PCR in conjunction with standard curves for detecting mRNA levels has previously been characterized by our laboratory and others [*19–21*].

**Table 1** Oligonucleotide sequences for RT-PCR analysis of gene expression of antioxidants and phase 2 enzymes in primary mouse cardiomyocytes

| **Enzymes** | **Primers** | |
|---|---|---|
| Catalase | Sense | GACATGGTCTGGGACTTCTG |
| | Antisense | GTAGGGACAGTTCACAGGTA |
| GCLC | Sense | GGAGGCTACTTCTGTACTA |
| | Antisense | CGATGGTCAGGTCGATGTCATT |
| GR | Sense | TGCCTGCTCTGGGCCATT |
| | Antisense | CTCCTCTGAAGAGGTAGGAT |
| GSTA1 | Sense | CCGTGCTTCACTACTTCAAT |

| | | |
|---|---|---|
| | Antisense | GCATCCATGGGAGGCTTTCT |
| GSTM1 | Sense | CTAGGAAGGGGAGTGCCTAA |
| | Antisense | CAGGCACTTGGGCTCAAACA |
| NQO1 | Sense | CCATTCTGAAAGGCTGGTTTG |
| | Antisense | CTAGCTTTGATCTGGTTGTC |
| HO-1 | Sense | GCCTTGAAGGAGGCCACCAA |
| | Antisense | CCTCAAACAGCTCAATGTTG |
| β-Actin | Sense | GACAACGGCTCCGGCATGT |
| | Antisense | GCAACATAGCACAGCTTCT |

Immunoblot Analysis of Antioxidative and Phase 2 Enzymes

The procedures described before [*13*] were followed to detect protein expression by immunoblot analysis. Briefly, cardiomyocytes were lysed by sonication followed by centrifugation to yield the supernatant samples. Equal amounts of protein from each of the samples were resolved by SDS-PAGE on 10% gels, and transferred electrophoretically to a nitrocellulose membrane (Amersham Biosciences, Piscataway, NJ). The membrane was blocked with 5% non-fat dried milk in TTBS buffer at room temperature for 1.5 h. The membrane was then incubated with the individual primary antibody overnight at 4°C, followed by incubation with a horseradish peroxidase-labeled secondary antibody (Santa Cruz Biotech, Santa Cruz, CA) at room temperature for another 1.5 h. The membrane was visualized using an enhanced chemiluminescence system (Amersham Biosciences), and the blots were quantified by Gel-Pro Analyzer version 4.5 (MediaCybernetics, Silver Spring, MD).

Assay for Cytotoxicity

Cytotoxicity was determined by a slightly modified 3-[4,5-dimethylthiazol-2-yl]-2,5-diphenyltetrazolium (MTT) reduction assay, as described before [*13*]. In brief, cardiomyocytes were plated into 48-well tissue culture plates. After incubation of the cells with the toxic agents in DMEM supplemented with 0.5% FBS at 37°C for 24 h, media were discarded, followed by addition to each well of 0.5 ml of fresh medium containing MTT (0.2 mg/ml). The plates were incubated at 37°C for another 2 h. Then, media were completely removed followed by addition to each well of 0.25 ml of mix of DMSO, isopropanol, and deionized water (1:4:5) to solubilize the formazan crystals. The amount of the dissolved formazan was then measured at 570 nm using a Beckman DU800 spectrophotometer.

Statistical Analysis

All data are expressed as means ± SEM from three separate experiments unless otherwise indicated. Differences between mean values of multiple groups were analyzed by one-way analysis of variance followed by Student-Newman-Keuls test. Differences between two groups were analyzed by Student *t*-test. Statistical significance was considered at $P \leq 0.05$.

## Results

Effects of Targeted Disruption of Nrf2 on Constitutive Levels/Activities of Antioxidants and Phase 2 Enzymes in Cardiomyocytes

We first examined if targeted disruption of Nrf2 affected the basal levels/activities of antioxidants and phase 2 enzymes in cardiomyocytes. As shown in Table 2, the basal levels/activities for all of the antioxidants and phase 2 enzymes examined were significantly lower in $Nrf2^{-/-}$ cardiomyocytes than in wild-type cells. Notably, targeted disruption of Nrf2 led to a 2.3- and 12.5-fold reduction in the basal activities of GST andNQO1, respectively, in cardiomyocytes. The levels/activities of other antioxidants and phase 2 enzymes, including SOD, catalase, GSH, GR, GPX, and HO, were reduced to various degrees, ranging from 20% to 38% decrease, in $Nrf2^{-/-}$ cardiomyocytes as compared to wild-type cells (Table 2).

**Table 2** Basal levels/activities of antioxidants and phase 2 enzymes in primary cardiomyocytes derived from $Nrf2^{-/-}$and wild-type ($Nrf2^{+/+}$) mice

| **Antioxidants/phase 2 proteins** | **$Nrf2^{+/+}$** | **$Nrf2^{-/-}$** |
|---|---|---|
| SOD (units/mg protein) | 2.4 ± 0.5 | 1.6 ± 0.4* |
| Catalase (μmol/min/mg protein) | 13.4 ± 1.7 | 10.7 ± 0.6* |
| GSH (nmol/mg protein) | 34.1 ± 0.9 | 21.1 ± 1.5* |
| GPx (nmol/min/mg protein) | 54.8 ± 6.5 | 37.8 ± 5.8* |
| GR (nmol/min/mg protein) | 56.2 ± 4.6 | 39.4 ± 2.5* |
| GST (nmol/min/mg protein) | 70.0 ± 3.5 | 30.5 ± 3.2* |
| NQO1 (nmol/min/mg protein) | 85.0 ± 20.4 | 6.8 ± 0.8* |
| HO (pmol/h/mg protein) | 288.5 ± 23.2 | 223.1 ± 32.5* |

Data represent means + SEM from three separate experiments. * significantly different from $Nrf2^{+/+}$ cells

Effects of Targeted Disruption of Nrf2 on Inducibility of SOD and Catalase by D3T in Cardiomyocytes

Incubation of either $Nrf2^{+/+}$ or $Nrf2^{-/-}$ cardiomyocytes with D3T (25–100 μM) for 24 h did not result in any significant changes in SOD activity (Fig. 1a). In contrast, such D3T treatment augmented catalase activity in $Nrf2^{+/+}$ cardiomyocytes; a nearly 2-fold induction of catalase activity was observed after treatment of $Nrf2^{+/+}$cells with 50 μM D3T. However, 100 μM D3T treatment did not cause any further induction of catalase activity in $Nrf2^{+/+}$ cardiomyocytes. The inducibility of catalase by D3T was not observed in $Nrf2^{-/-}$ardiomyocytes; instead, a significant decrease in catalase activity was found in the $Nrf2^{-/-}$ cells after treatment with 100 μM D3T (Fig. 1b). Immunoblot analysis revealed that D3T treatment of $Nrf2^{+/+}$cardiomyocytes increased the protein level of catalase in a concentration-dependent manner, with the highest induction of catalase protein expression observed after treatment with 100 μM D3T. The D3T-mediated induction of catalase protein expression was completely abolished in $Nrf2^{-/-}$ cardiomyocytes (Fig. 1c and d).

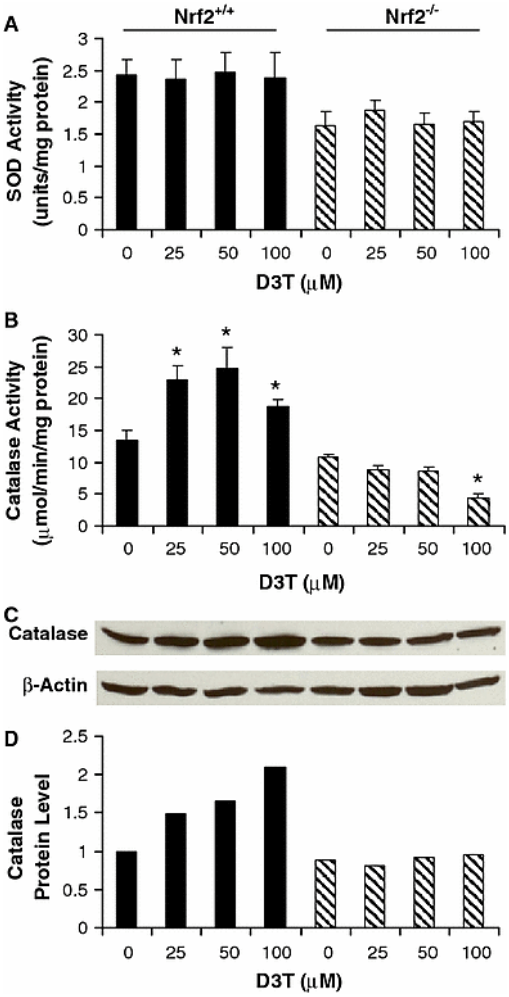

**Fig. 1** Effects of D3T treatment on SOD and catalase activities, as well as catalase protein expression in Nrf2$^{+/+}$and Nrf2$^{-/-}$ cardiomyocytes. Cardiomyocytes were incubated with the indicated concentrations of D3T for 48 h, followed by measurement of cellular SOD and catalase activity, as well as catalase protein expression. Values in panels A and B represent means ± SEM from three separate experiments. Immunoblot gel pictures in panel C are representative of two separate experiments. Values in panel D represent averages of data from two separate experiments, and the data are expressed as relative ratios of density of the catalase protein bands after normalization to that of β-actin. *, significantly different from 0 μM D3T

Effects of Targeted Disruption of Nrf2 on Inducibility of GSH and γ-Glutamylcysteine Ligate (γGCL) by D3T in Cardiomyocytes

Treatment of Nrf2$^{+/+}$ cardiomyocytes with D3T (25–100 μM) led to a 2–3-fold induction of cellular GSH content in a concentration-dependent fashion. A 30% increase in GSH content was also observed in Nrf2$^{-/-}$cardiomyocytes after treatment with 100 μM D3T (Fig. 2a).
In Nrf2$^{+/+}$ cardiomyocytes, the protein level of γGCL, the rate-limiting enzyme in GSH synthesis, was also remarkably induced by D3T in a concentration-dependent relationship. However, no significant induction of γGCL protein by D3T was observed in Nrf2$^{-/-}$cardiomyocytes (Fig. 2b and c).

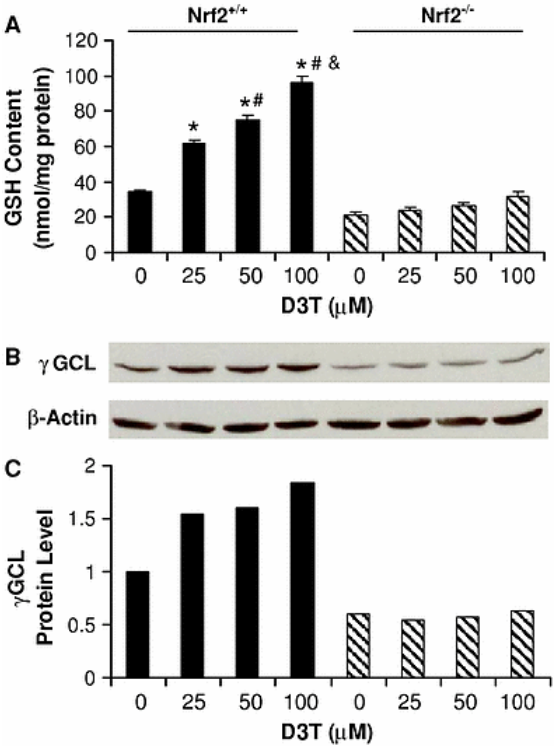


**Fig. 2** Effects of D3T treatment on GSH content and γGCL protein expression in Nrf2$^{+/+}$ and Nrf2$^{-/-}$cardiomyocytes. Cardiomyocytes were incubated with the indicated concentrations of D3T for 48 h, followed by measurement of cellular GSH content, and γGCL

protein expression. Values in panel A represent means ± SEM from three separate experiments. Immunoblot gel pictures in panel B are representative of two separate experiments. Values in panel C represent averages of data from two separate experiments, and the data are expressed as relative ratios of density of the γGCL protein bands after normalization to that of β-actin. *, significantly different from 0 μM D3T; #, significantly different from 25 μM D3T; &, significantly different from 50 M D3T

Effects of Targeted Disruption of Nrf2 on Inducibility of GPx and GR by D3T in Cardiomyocytes

Wild-type cardiomyocytes expressed basal activities of GPx and GR, similar to those found in most other types of cells. Although the basal activity of GPx in $Nrf2^{-/-}$ cardiomyocytes was lower than that in wild-type cells, treatment of either type of cells with D3T led to significant induction of GPx activity; an overall 20–30% induction of the enzyme was observed in both $Nrf2^{+/+}$ and $Nrf2^{-/-}$ cardiomyocytes after treatment with D3T (25–100 μM) (Fig. 3a). In contrast to GPx, GR in $Nrf2^{+/+}$ cardiomyocytes was more inducible by D3T; a 30–100% induction of GR activity was found after treating these cells with D3T at 25–100 μM. The induction of GR by D3T in wild-type cardiomyocytes was dependent on the concentrations of D3T. Similarly, immunoblot analysis showed a D3T concentration-dependent induction of GR protein expression in $Nrf2^{+/+}$cardiomyocytes (Fig. 3c and d). In contrast, neither GR activity nor its protein level was induced by D3T in$Nrf2^{-/-}$ cardiomyocytes.

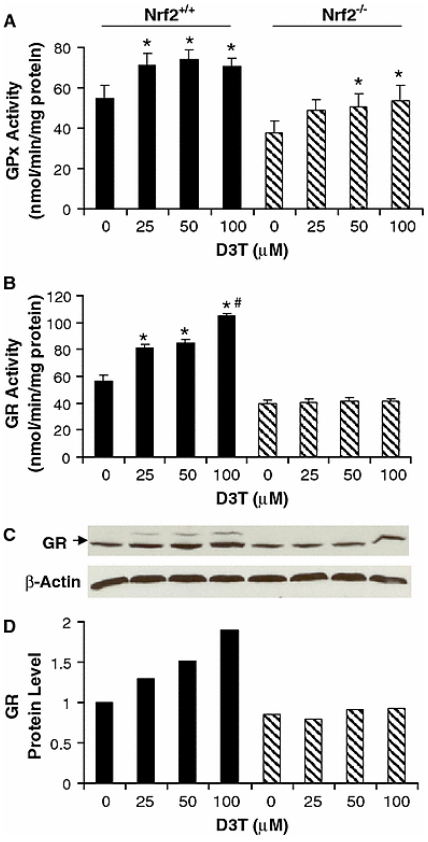

**Fig. 3** Effects of D3T treatment on GPx and GR activities, as well as GR protein expression in $Nrf2^{+/+}$ and $Nrf2^{-/-}$cardiomyocytes. Cardiomyocytes were incubated with the indicated concentrations of D3T for 48 h, followed by measurement of cellular GPx and GR activity, as well as GR protein expression. Values in panels A and B represent means ± SEM from three separate experiments. Immunoblot gel pictures in panel C are representative of two separate experiments. Values in panel D represent averages of data from two separate experiments, and the data are expressed as relative ratios of density of the GR protein bands after normalization to that of β-actin. *, significantly different from 0 μM D3T; #, significantly different from 25 μM D3T

Effects of Targeted Disruption of Nrf2 on Inducibility of GST and its Major Isozymes by D3T in Cardiomyocytes

GST exists as a family of various isozymes, including GST-A, -M, and -P in mammalial cells [*22*]. As shown in Fig. 4, cardiomyocytes expressed constitutively a measurable total GST activity as well as the three major isozyme proteins. The total GST activity in $Nrf2^{+/+}$ cardiomyocytes was highly inducible by D3T in a concentration-dependent manner. The induction of GST activity was completely lost in $Nrf2^{-/-}$cardiomyocytes (Fig. 4a). The basal protein levels of GST-A and -M, but not -P, were also significantly lower in $Nrf2^{-/-}$ cardiomyocytes than in wild-type cells. Similar to the D3T-inducibility of total GST activity in $Nrf2^{+/+}$cardiomyocytes, the protein levels of GST-A and -M in these cells were also highly inducible by D3T in a concentration-dependent relationship. Targeted disruption of Nrf2 led to a complete abolishment of the D3T inducibility of the total GST activity as well as the protein expression of the A and M isozymes (Fig. 4b–d).
Both $Nrf2^{+/+}$ and $Nrf2^{-/-}$ cardiomyocytes showed a similar basal level of GST-P protein. The protein level of this GST isozyme was not altered by D3T treatment in either $Nrf2^{+/+}$ or $Nrf2^{-/-}$ cardiomyocytes (Fig. 4e).

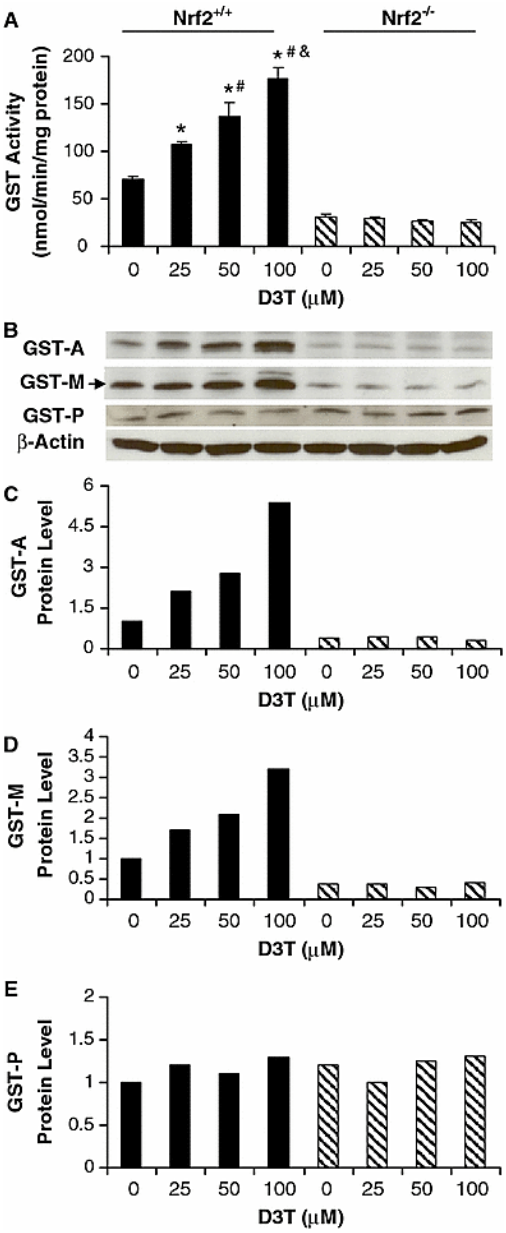


**Fig. 4** Effects of D3T treatment on total GST activity and the protein expression of GST-A, GST-M, and GST-P in $Nrf2^{+/+}$ and $Nrf2^{-/-}$ cardiomyocytes. Cardiomyocytes were incubated with the indicated concentrations of D3T for 48 h, followed by measurement of total cellular GST activity, as well as the protein expression of GST-A, -M, and -P. Values in panel A represent means ± SEM from three separate experiments. Immunoblot gel pictures in panel B are representative of two separate experiments. Values in panels C-E represent averages of data from two separate experiments, and the data are expressed as relative ratios of density of the respective GST isozyme protein bands after normalization to that of β-actin. *, significantly different from 0 μM D3T; #, significantly different from 25 μM D3T; &, significantly different from 50 μM D3T

Effects of Targeted Disruption of Nrf2 on Inducibility of NQO1 by D3T in Cardiomyocytes

NQO1 is probably the most inducible phase 2 enzyme in mammalian cells. As shown in Fig. 5, incubation of $Nrf2^{+/+}$ cardiomyocytes with D3T (25–100 μM) resulted in a remarkable 4–11-fold induction of NQO1 activity as well as the protein expression of this phase 2 enzyme. Targeted disruption of Nrf2 in cardiomyocytes not only led to a dramatic reduction of the basal activity of NQO1 (Table 2), also a complete abolishment of its inducibility by D3T (Fig. 5).

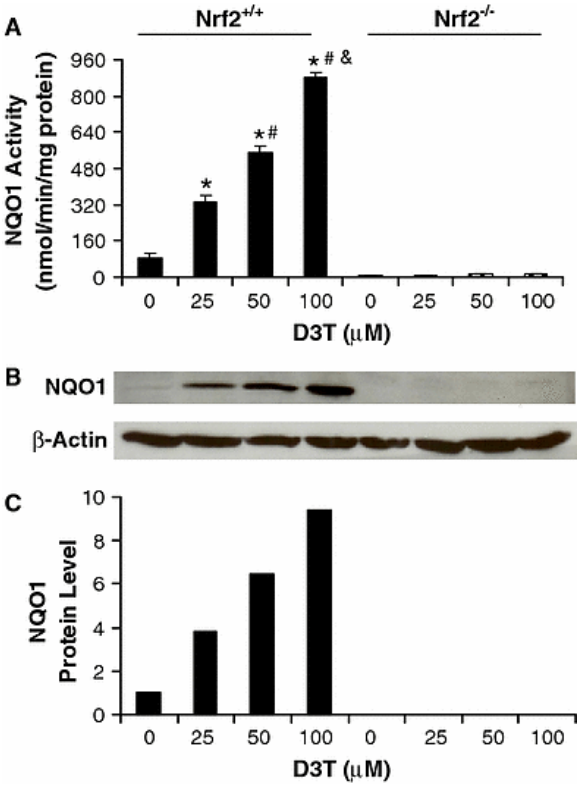


**Fig. 5** Effects of D3T treatment on NQO1 activity and protein expression in $Nrf2^{+/+}$ and $Nrf2^{-/-}$ cardiomyocytes. Cardiomyocytes were incubated with the indicated concentrations of D3T for 48 h, followed by measurement of cellular NQO1 activity and protein expression. Values in panel A represent means ± SEM from three separate experiments. Immunoblot gel pictures in panel B are representative of two separate experiments. Values in panel C represent averages of data from two separate experiments, and the data are expressed as relative ratios of density of the NQO1 protein bands after normalization to that of β-actin. *, significantly different from 0 μM D3T; #, significantly different from 25 μM D3T; &, significantly different from 50 μM D3T

Effects of Targeted Disruption of Nrf2 on Inducibility of HO by D3T in Cardiomyocytes

HO exists in two major isoforms, HO-1 and HO-2, with HO-1 being inducible under various stress and inflammatory conditions [*23*, *24*]. We observed that treatment of wild-type cardiomyocytes with D3T caused a concentration-dependent increase in the activity of HO, as

determined by metabolism of heme to eventually form bilirubin. An 80% increase in HO activity was found in wild-type cardiomyocytes after treatment with 100 μM D3T. Induction of HO activity by D3T was not observed in $Nrf2^{-/-}$ cardiomyocytes (Fig. 6a). Immunoblot assay revealed that the basal protein level of HO-1 was also reduced in $Nrf2^{-/-}$cardiomyocytes as compared to wild-type cells. The protein level of HO-1 in $Nrf2^{+/+}$ cardiomyocytes was remarkably increased by D3T treatment; a 70, 100, and 120% increase of HO-1 protein expression was observed after treatment of the $Nrf2^{+/+}$ cells with 25, 50, and 100 μM D3T, respectively (Fig. 6b and c).

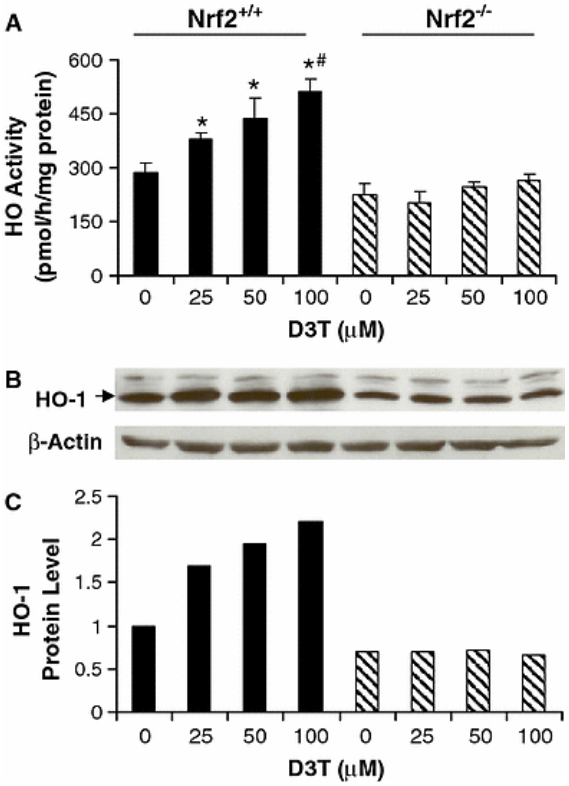


**Fig. 6** Effects of D3T treatment on HO activity and protein expression of HO-1 in $Nrf2^{+/+}$ and $Nrf2^{-/-}$cardiomyocytes. Cardiomyocytes were incubated with the indicated concentrations of D3T for 48 h, followed by measurement of cellular HO activity and protein expression of HO-1. Values in panel A represent means ± SEM from three separate experiments. Immunoblot gel pictures in panel B are representative of two separate experiments. Values in panel C represent averages of data from two separate experiments, and the data are expressed as relative ratios of density of the HO-1 protein bands after normalization to that of β-actin. *, significantly different from 0 μM D3T; #, significantly different from 25 μM D3T

Effects of Targeted Disruption of Nrf2 on Inducibility by D3T of mRNA Levels for Various Antioxidative and Phase 2 Enzyme Genes in Cardiomyocytes

Since D3T-mediated induction of catalase, GSH/γGCL, GR, GST-A, GST-M, NQO1, and HO/HO-1 was dependent on the status of Nrf2 (Figs. 1–6), we next examined the effects of targeted disruption of Nrf2 on D3T-inducible expression of mRNA for the above antioxidative and phase 2 enzymes. As shown in Fig. 7, D3T treatment led to significant time-dependent increases in the levels of mRNA for catalase, γGCL catalytic subunit (GCLC), GR, GST-A1, GST-M1, NQO1, and HO-1 in wild-type, but not $Nrf2^{-/-}$cardiomyocytes. Notably, the basal levels of mRNA for GCLC, GST-A1, and NQO1 were also reduced in$Nrf2^{-/-}$ cardiomyocytes as compared to wild-type cells. Although the basal activities and/or protein expression of catalase, GR, GST-M, HO/HO-1 were reduced in $Nrf2^{-/-}$ cardiomyocytes, the basal mRNA levels for catalase, GR, GST-M1, and HO-1 were not altered by targeted disruption of Nrf2 (Fig. 7).

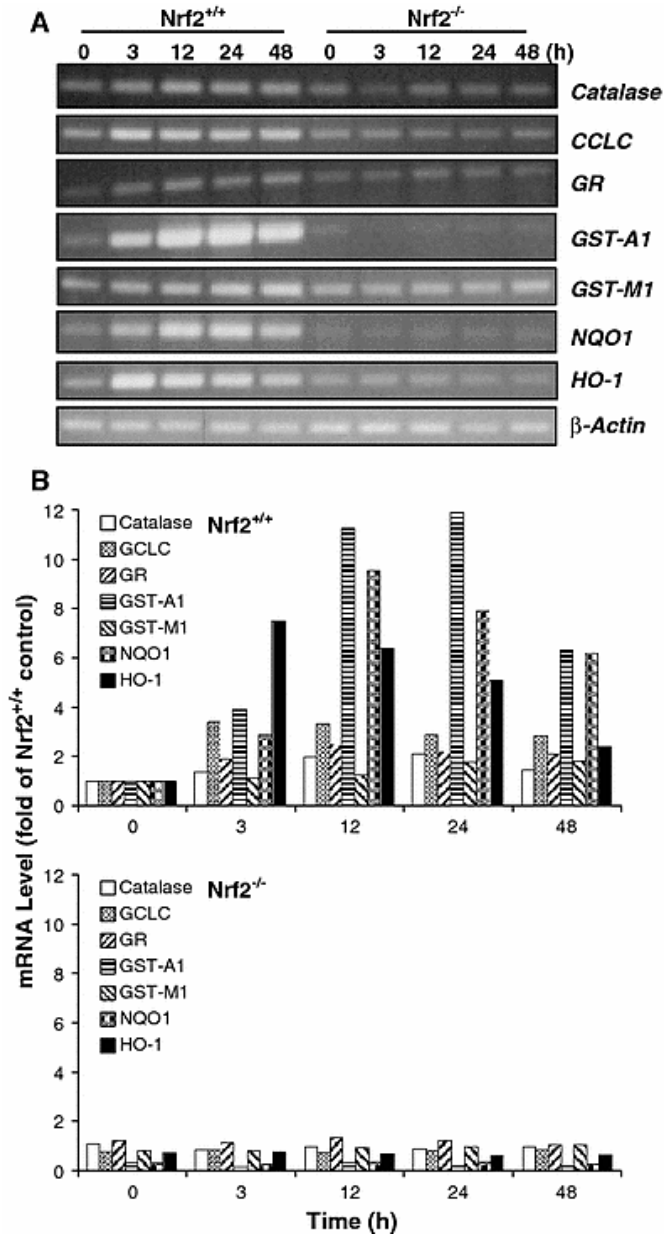

**Fig. 7** Effects of D3T treatment on mRNA expression of various antioxidative and phase 2 genes in $Nrf2^{+/+}$ and$Nrf2^{-/-}$ cardiomyocytes. Cardiomyocytes were incubated with 100 μM D3T for the indicated time points, followed by detection of cellular mRNA levels for the indicated genes. RT-PCR gel pictures in panel A are representative of two separate experiments. Values in panel B represent averages of data from two separate experiments, and the data are expressed as relative ratios of density of the gel DNA bands for the respective genes after normalization to that of β-actin

Effects of Targeted Disruption of Nrf2 on Susceptibility of Cardiomyocytes to Oxidative and Electrophilic Injury as well as the Myocardiac Cytoprotective Effects of D3T

$H_2O_2$ is one of the most commonly encountered reactive oxygen in causing oxidative biological damage, including myocardiac cell injury. As shown in Fig. 8a, $Nrf2^{-/-}$ cardiomyocytes showed increased sensitivity to $H_2O_2$-induced cell injury, as compared to wild-type cells. Pretreatment of wild-type cardiomyocytes with D3T afforded a marked cytoprotection against $H_2O_2$-medicated cell injury; the cytoprotection was remarkable at all of the toxic concentrations of $H_2O_2$ used (100, 150, 200, and 250 μM). However, D3T pretreatment under the same conditions led to no significant cytoprotection against $H_2O_2$-mediated cell injury in $Nrf2^{-/-}$cardiomyocytes. Exposure of either $Nrf2^{+/+}$ or $Nrf2^{-/-}$ cardiomyocytes to 200 μM $H_2O_2$ also caused significant changes in cell morphology, as indicated by extensive cell shrinkage, loss of cell processes, and presence of cell debris (Fig. 9). D3T pretreatment of the wild-type cardiomyocytes prevented the above cell morphological changes. However, the same D3T pretreatment of $Nrf2^{-/-}$ cardiomyocytes afforded no protection against $H_2O_2$-induced morphological damage (Fig. 9). As compared to wild-type cells, $Nrf2^{-/-}$cardiomyocytes also exhibited increased susceptibility to cell injury induced by various concentrations of SIN-1, a generator of peroxynitrite, which is a potent oxidant in biological systems [*25*] (Fig. 8b). Pretreatment of wild-type cardiomyocytes with D3T afforded a dramatic cytoprotection against SIN-1-induced cell injury. Notably, a remarkable cytoprotection by D3T pretreatment was seen at all of the four toxic concentrations (400, 600, 800, and 1,000 μM) of SIN-1. In contrast, pretreatment of $Nrf2^{-/-}$ cardiomyocytes with the same concentration of D3T led to no cytoprotection against SIN-1-induced cell injury (Fig. 8b). As shown in Fig. 9, the cell morphological damage (extensive cell shrinkage, loss of cell processes, and presence of cell debris) induced by 800 μM SIN-1 was prevented in D3T-pretreated $Nrf2^{+/+}$ cardiomyocytes; whereas the above cell morphological damage was not protected by D3T pretreatment of the $Nrf2^{-/-}$cardiomyocytes (Fig. 9).

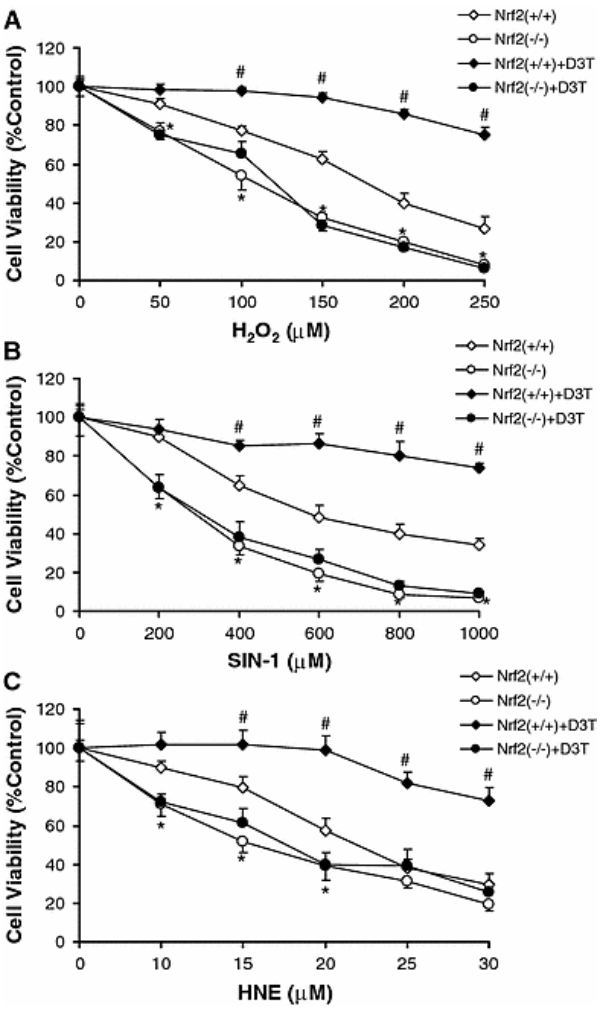


**Fig. 8** Oxidative and electrophilic species-induced cytotoxicity in $Nrf2^{+/+}$ and $Nrf2^{-/-}$ cardiomyocytes, and the cytoprotective effects of D3T pretreatment. Cardiomyocytes were incubated with or without 100 μM D3T for 48 h, followed by incubation with various concentrations of $H_2O_2$, SIN-1, or HNE for another 24 h. After this incubation, cytotoxicity was determined by MTT reduction assay. Values represent means ± SEM from three separate experiments. *, significantly different from Nrf2(+/+); #, significantly different from Nrf2(+/+)

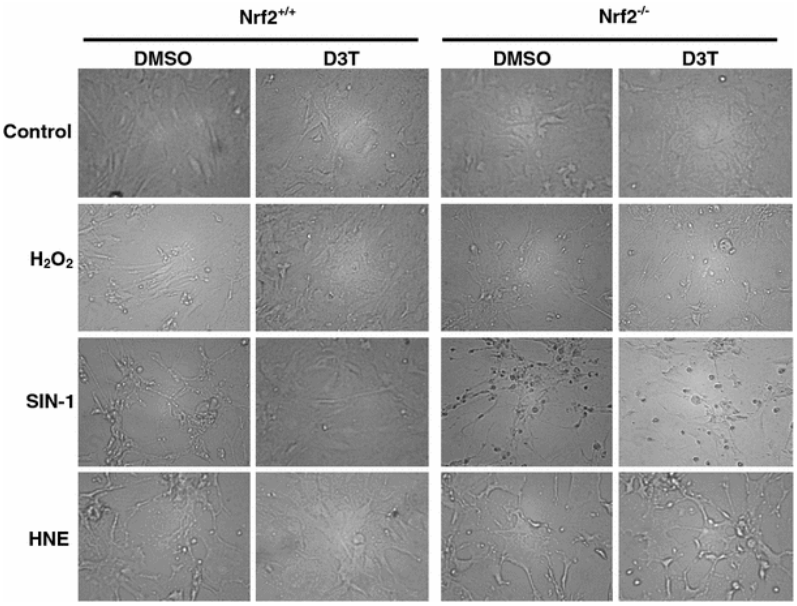


**Fig. 9** Oxidative and electrophilic species-induced cell morphological changes in $Nrf2^{+/+}$ and $Nrf2^{-/-}$cardiomyocytes, and the cytoprotective effects of D3T pretreatment. Cardiomyocytes were incubated with or without 100 M D3T for 48 h, followed by incubation with 200 μM $H_2O_2$, 800 M SIN-1, or 25 μM HNE for another 24 h. After this incubation, cell injury was assessed by examining the morphological changes under light microscopy

To investigate the role of Nrf2 in determining the susceptibility of cardiomyocytes to electrophilic stress, we exposed to the cardiomyocytes to 4-hydroxy-2-nonenal (HNE), a potent electrophilic species involved in cardiac disorders, including myocardial ischemia-reperfusion injury [*26*, *27*]. As shown in Fig. 8c, targeted disruption of Nrf2 dramatically sensitized the cardiomyocytes to HNE-induced cell injury. Exposure of wild-type cardiomyocytes to HNE at 15, 20, 25, and 30 μM also led to significant concentration-dependent decreases in cell viability, and the cell injury induced by the above concentrations of HNE was greatly protected by D3T pretreatment. However, the same D3T pretreatment of $Nrf2^{-/-}$ cardiomyocytes led to no significant cytoprotection against HNE-induced cell injury (Fig. 8c). Similarly, the HNE-induced cell morphological changes (extensive cell shrinkage, loss of cell processes, and presence of cell debris) were prevented by D3T pretreatment in wild-type, but not $Nrf2^{-/-}$ cardiomyocytes (Fig. 9).

## Discussion

Although it is widely recognized that Nrf2 signaling is indispensable for regulation of a number of cytoprotective genes in mammalian tissues, including liver and lung [*11*, *12*, *28*], its role in controlling either constitutive or inducible expression of a series of antioxidants and phase 2 enzymes in primary cardiomyocytes remains unknown. A number of studies demonstrate that the exact role of Nrf2 signaling in regulating individual antioxidative and phase 2 genes varies among different types of cells or tissues [*13*,*28–30*]. Thus, it is of importance to investigate the

involvement of this critical transcriptional activator in regulating myocardiac cellular antioxidants and phase 2 enzymes, and in controlling the susceptibility of cardiomyocytes to oxidative and electrophilic stress as well as myocardiac cytoprotection by chemoprotectants capable of modulating cellular antioxidative and phase 2 enzyme defenses. The results of this study demonstrated that the constitutive levels/activities of a series of important antioxidants and phase 2 enzymes in primary cardiomyocytes were dependent on the status of Nrf2. While the exact underlying mechanisms remain to be elucidated, the reduced levels/activities of antioxidants and phase 2 enzymes in $Nrf2^{-/-}$ cardiomyocytes could be due to either a decrease in Nrf2-mediated ARE-driven transcriptional activation, or an indirect effect of the altered cellular redox state. The later mechanism seemed to be in line with the observation that despite the reduced basal activities/protein expression of some of the enzymes, including catalase, GR, and HO-1 in $Nrf2^{-/-}$ cardiomyocytes, the mRNA levels for these enzyme genes were not altered by the deletion of Nrf2 under the present experimental conditions (Fig. 7).

Nrf2 signaling controls inducible expression of a large number of cytoprotective genes. However, studies on the involvement of Nrf2 in regulating the inducible expression of cellular catalase and SOD have yielded inconsistent conclusions. The results of this study showed that basal activities of both SOD and catalase were reduced in $Nrf2^{-/-}$ cells (Table 2), treatment of cardiomyocytes with D3T caused significant induction of catalase, but not SOD, and the induction of catalase by D3T was dependent on Nrf2 (Fig. 1). We previously found that in cardiac fibroblasts both SOD and catalase were inducible by D3T in an Nrf2-dependent manner [*30*]. Thus, in different types of cells within even the same tissue Nrf2 appeared to play different roles in regulating the inducible expression of SOD. Induction of catalase protein expression by D3T in cardiomyocytes showed a concentration-dependency; however the further increased catalase protein level in 100 μM D3T treated wild-type cardiomyocytes (Fig. 1c and d) did not result in an additional increase in the enzyme activity (Fig. 1b), suggesting that a higher concentration (100 μM) of D3T exerted a negative effect on catalase activity. This notion was also consistent with the observation that in $Nrf2^{-/-}$ cardiomyocytes, 100 μM D3T caused a significant decrease in catalase activity without affecting its protein level (Fig. 1b–d). It remains unclear how 100 μM D3T suppressed catalase activity in $Nrf2^{-/-}$ cardiomyocytes.

In contrast to SOD and catalase, the involvement of Nrf2 signaling in regulating cellular GSH is well established [*11–13*]. The induction of GSH by D3T was dramatically diminished in $Nrf2^{-/-}$ cardiomyocytes (Fig. 2), suggesting that Nrf2 was largely responsible for regulating D3T-mediated increase of cellular GSH content. D3T-mediated induction of γGCL, the key enzyme in GSH biosynthesis, was completely diminished in $Nrf2^{-/-}$ cardiomyocytes, suggesting that D3T-mediated elevation of cellular GSH occurred via Nrf2-dependent upregulation of γGCL. In this regard, the mRNA level for GCLC, the subunit that determines the catalytic activity of the γGCL enzyme complex [*31*], was also increased by D3T treatment in an Nrf2-dependent manner (Fig. 7). In $Nrf2^{-/-}$ cardiomyocytes, 100 μM D3T also significantly increased cellular GSH content, but not γGCL protein level (Fig. 2). This observation suggested that

elevation of GSH by D3T in Nrf2 $^{-/-}$cardiomyocytes might occur via a γGCL-independent mechanism. Regardless of the increased level of GSH in 100 μM D3T-treated Nrf2$^{-/-}$ cardiomyocytes, the complete abolishment of D3T-mediated induction of γGCL protein and mRNA expression by targeted disruption of Nrf2 (Figs. 2 and 7) demonstrated that Nrf2 signaling was critical for D3T-mediated induction of γGCL, and the subsequent elevation of cardiomyocyte GSH content. One notable observation of this study was the similar induction of GPx activity by D3T in both Nrf2$^{-/-}$ and wild-type cardiomyocytes (Fig. 3). GPx exists as a family of at least six isozymes (GPx1-6), with GPx1 and GPx4 widely distributed in mammalian tissues/cells. It is known that the gastrointestinal form of GPx (GPx2) is regulated by Nrf2 signaling. In this regard, an ARE is identified in the promoter region of GPx2 gene [*32*]. The similar degree of GPx induction by D3T in Nrf2$^{+/+}$ and Nrf2$^{-/-}$ cardiomyocytes indicated that the inducible expression of the ubiquitous forms of GPx (GPx1 and 2) in cardiomyocytes were independent of Nrf2 regulation. Similar to what was observed with GSH, D3T also potently induced GR activity as well as its protein and mRNA expression in wild-type, but not Nrf2$^{-/-}$ cardiomyocytes (Figs. 3 and7), pointing to a critical role for Nrf2 in regulating the inducible expression of GR in cardiomyocytes. The above observations were also in line with previous studies, demonstrating that both γGCL and GR are Nrf2-regulated antioxidant genes [*13*, *28–30*].

Among the various cytoprotective proteins GST and NQO1 are the two most extensively investigated Nrf2-regulated phase 2 enzymes [*11–13*, *28–30*]. The constitutive and inducible expression of these two phase 2 enzymes and their regulation by Nrf2 pathway in primary cardiomyocytes have not been reported in the literature. The dramatic decreases in the basal activities of GST and NQO1 in Nrf2$^{-/-}$ cells (Table 2) indicated that Nrf2 signaling was critical for regulating the constitutive expression of these two phase 2 enzymes in cardiomyocytes. The complete abolishment of the D3T-inducibility of total GST activity in Nrf2$^{-/-}$cells suggested that Nrf2 was also an indispensable factor in regulating not only the basal activity but also the inducible expression of GST in cardiomyocytes. GST exists as a family of various isozymes, with GST-A, -M, and -P being the three major isozymes in most types of cells [*22*]. It is important to note that the expression of the above GST isoforms, their differential induction by chemoprotectants, as well as the role of Nrf2 in their regulation in cardiomyocytes have not been investigated. Our results demonstrated that along with induction of the total cellular GST activity, D3T treatment also led to significant increases in the protein levels of GST-A and -M, as well as the mRNA levels of GST-A1 and -M1 in wild-type, but not Nrf2$^{-/-}$cardiomyocytes (Figs. 4 and 7). Notably, treatment of either wild-type or Nrf2$^{-/-}$ cardiomyocytes with D3T did not result in any changes in the protein level of GST-P (Fig. 4). Previous studies also showed that GST-P was not readily inducible by chemoprotectants, including D3T in various types of cells [*13*, *33*]. It is also possible that different isozymes of GST in cardiomyocytes were regulated differently by the Nrf2 pathway. The remarkable induction (up to 11-fold) of NQO1 by D3T in Nrf2$^{+/+}$ cardiomyocytes (Fig. 5) was unexpected. This observation may have important implications in cardioprotection in view of the recent observations thatNQO1 is not only capable

of detoxifying electrophilic quinones, but also acting as an antioxidative enzyme, a scavenger of superoxide, as well as a p53-stabilizing protein [*34–37*].

Another important observation of this study was the potent induction of HO/HO-1 by D3T in cardiomyocytes that occurred in an Nrf2-dependent relationship (Figs. 6 and 7). HO-1 has been recently demonstrated to play a crucial role in defending cells against oxidative and inflammatory stress. In this context, HO-1 overexpression is found to be protective against various forms of cardiovascular diseases, including atherosclerosis and myocardial ischemia-reperfusion injury [*23*, *24*, *38*, *39*]. The significant induction of HO/HO-1 by D3T in cardiomyocytes via an Nrf2-dependent mechanism may thus be an important pathway for myocardiac cytoprotection against oxidative and inflammatory injury.

Studies over the last two decades have demonstrated that oxidative and electrophilic stress as well as dysregulated inflammation are intimately involved in the pathophysiological processes of various cardiac diseases [*1–4*]. Accordingly, upregulation of endogenous antioxidants and phase 2 enzymes may represent an effective strategy for myocardiac cytoprotection against oxidative and electrophilic injury. To investigate if Nrf2-dependent regulation of endogenous cellular antioxidative and phase 2 defenses plays an important part in myocardiac cytoprotection, cardiomyocytes were exposed to various oxidative and electrophilic species, including $H_2O_2$, SIN-1-derived peroxynitrite, and HNE. $H_2O_2$ and peroxynitrite are the most encountered oxidants in biological systems. Indeed, these oxidative species have been found to be responsible for injury of cardiomyocytes in various cardiac disorders, such as myocardial ischemia-reperfusion injury [*1–4*]. As expected, cell injury induced by $H_2O_2$ or SIN-1-derived peroxynitrite was markedly augmented in $Nrf2^{-/-}$ cardiomyocytes, and D3T-treatment of the wild-type, but not $Nrf2^{-/-}$, cardiomyocytes provided a remarkable cytoprotection against these oxidant-induced cell injury (Figs. 8 and 9). It is known that detoxification of $H_2O_2$ in mammalian cells relies on several cellular antioxidants, especially GSH (in the presence of GPx) and catalase. GSH in the presence of GPx has also been found to be a major cellular mechanism for detoxification of peroxynitrite [*40*]. In addition, the augmented activity of GR by D3T could also contribute to the increased levels of GSH due to its ability to reduce GSSG to GSH. Therefore, the reduced constitutive expression of the above antioxidants as well as their inability to be upregulated by D3T in $Nrf2^{-/-}$ cardiomyocytes were most likely responsible for the increased susceptibility of these cells to the above oxidant-elicited cell injury. The increased resistance of the D3T-treated $Nrf2^{+/+}$cardiomyocytes to oxidative stress may also result partially from the potent induction of HO-1 by D3T (Figs. 6 and 7). HO-1 catalyzes the decomposition of heme to produce the potent antioxidant, bilirubin and the anti-inflammatory/antioxidative molecule, carbon monoxide [*23*, *24*]. Overexpression of HO-1 has been demonstrated extensively to protect cells, including cardiomyocytes from oxidative injury [*23*, *24*].

In addition to its direct involvement in detoxification of oxidants, GSH is also a cofactor for GST, an abundant cellular enzyme primarily involved in the detoxification of electrophilic compounds via catalyzing the formation of GSH-electrophile conjugates [*22*]. Several recent

studies have demonstrated that GST also plays a critical role in protecting cells from oxidant-mediated injury through catalyzing the decomposition of lipid hydroperoxides generated from oxidative damage of cellular lipid molecules [*41*, *42*]. Accordingly, the marked induction of GST by D3T in $Nrf2^{+/+}$ cardiomyocytes may also contribute partially to the increased resistance of the D3T-treated cells to the oxidant-elicited cytotoxicity.

As mentioned above, NQO1 not only detoxifies electrophilic quinones but also plays a critical role in controlling oxidative stress via maintaining high levels of cellular vitamin E and ubiquinol, two important antioxidants [*34*]. This is particularly relevant for the involvement of NQO1 in protecting against oxidative myocardiac cell injury in view of the extremely high D3T-inducible expression of this phase 2 enzyme in $Nrf2^{+/+}$ cardiomyocytes (Fig. 5).

Targeted disruption of Nrf2 augmented the susceptibility of cardiomyocytes to HNE-induced cell injury (Figs. 8 and 9). HNE is a potent electrophilic, α, β-unsaturated aldehyde, which is formed during lipid peroxidation in biological systems [*43*]. HNE has been implicated in the pathogenesis of various cardiac disorders, including myocardial ischemia-reperfusion injury [*26*, *27*]. Although a number of cellular factors have been proposed to participate in metabolism of HNE in biological systems, detoxification of HNE heavily relies on cellular GSH system in mammalian cells [*22*, *44*]. In this context, due to its high electrophilic property, HNE readily reacts with GSH to form a less reactive GSH-conjugate, leading to its detoxification [*22*]. The presence of GST has also been found to promote the conjugation reaction between HNE and GSH [*22*, *45*]. Thus, the decreased level/activity of GSH/GST and their inability to be induced by D3T would account for the augmented sensitivity of the $Nrf2^{-/-}$ cardiomyocytes to HNE-induced cell injury and for the failure of D3T treatment to protect these cells from HNE toxicity.

In summary, the results of the present study demonstrate that Nrf2 is indispensable for the regulation of both constitutive and D3T-inducible expression of a series of key antioxidants and phase 2 enzymes in mouse primary cardiomyocytes. Nrf2 signaling is also an important mechanism in controlling cardiomyocyte susceptibility to cell injury elicited by various oxidative and electrophilic species. In view of the crucial involvement of oxidative and electrophilic injury of cardiomyocytes in the pathophysiological processes of various cardiac disorders, Nrf2-dependent coordinated regulation of a series of antioxidants and phase 2 enzymes in these cells is of importance in protecting against the pathogenesis underlying cardiac diseases. The results of this study implicate Nrf2 signaling pathway as an important mechanism for myocardiac cytoprotection.

## Acknowledgments

This work was supported by grant R01HL71190 from the National Institutes of Health and a grant from Harvey Peters Research Foundation (YL).

## References

1. McCord, J. M. (1985). Oxygen-derived free radicals in postischemic tissue injury. *The New England Journal of Medicine, 312,* 159–163.

2. Villamena, F. A., & Zweier, J. L. (2004). Detection of reactive oxygen, nitrogen species by EPR spin trapping. *Antioxidants & Redox Signaling, 6,* 619–629. doi:10.1089/152308604773934387.

3. Kutala, V. K., Khan, M., Angelos, M. G., & Kuppusamy, P. (2007). Role of oxygen in postischemic myocardial injury. *Antioxidants & Redox Signaling, 9,* 1193–206. doi:10.1089/ars.2007.1636.

4. Kang, Y. J. (2007). Antioxidant defense against anthracycline cardiotoxicity by metallothionein. *Cardiovascular Toxicology, 7,* 95–100 doi:10.1007/s12012-007-0007-3.

5. Salvemini, D., Wang, Z. Q., Zweier, J. L., Samouilov, A., Macarthur, H., Misko, T. P., Currie, M. G., Cuzzocrea, S., Sikorski, J. A., & Riley, D. P. (1999). A nonpeptidyl mimic of superoxide dismutase with therapeutic activity in rats. *Science, 286,* 304–306. doi:10.1126/science.286.5438.304.

6. Lefer, D. J., & Granger, N. (2000). Oxidative stress and cardiac disease. *The American Journal of Medicine, 109,* 315–323. doi:10.1016/S0002-9343(00)00467-8.

7. Steinberg, D. (2002). Atherogenesis in perspective: Hypercholesterolemia and inflammation as partners in crime. *Nature Medicine, 8,* 1211–1217. doi:10.1038/nm1102–1211.

8. Bolli, R., Becker, L., Gross, G., Mentzer, R. Jr., Balshaw, D., & Lathrop, D. A. (2004). NHLBI working group on the translation of therapies for protecting the heart from ischemia. Myocardial protection at a crossroads: The need for translation into clinical therapy. *Circulation Research, 95,* 125–134. doi:10.1161/01.RES.0000137171.97172.d7.

9. Lonn, E., Bosch, J., Yusuf, S., Sheridan, P., Pogue, J., Arnold, J. M., Ross, C., Arnold, A., Sleight, P., Probstfield, J., & Dagenais, G. R. (2005). HOPE and HOPE-TOO trial investigators. Effects of long-term vitamin E supplementation on cardiovascular events and cancer: A randomized controlled trial. *Journal of the American Medical Association, 293,* 1338–1347. doi:10.1001/jama.293.11.1338.

10. Bailey, D. M., Raman, S., McEneny, J., Young, I. S., Parham, K. L., Hullin, D. A., Davies, B., McKeeman, G., McCord, J. M., & Lewis, M. H. (2006). Vitamin C prophylaxis promotes oxidative lipid damage during surgical ischemia-reperfusion. *Free Radical Biology & Medicine, 40,* 591–600. doi:10.1016/j.freeradbiomed.2005.09.024.

11. Itoh, K., Chiba, T., Takahashi, S., Ishii, T., Igarashi, K., Katoh, Y., Oyake, T., Hayashi, N., Satoh, K., Hatayama, I., Yamamoto, M., & Nabeshima, Y. (1997). An Nrf2/small Maf heterodimer mediates the induction of phase II detoxifying enzyme genes through antioxidant

response elements. *Biochemical and Biophysical Research Communications, 236*, 313–322. doi:10.1006/bbrc.1997.6943.

12. Motohashi, H., & Yamamoto, M. (2004). Nrf2-Keap1 defines a physiologically important stress response mechanism. *Trends in Molecular Medicine, 10*, 549–557. doi:10.1016/j.molmed.2004.09.003.

13. Zhu, H., Zhang, L., Itoh, K., Yamamoto, M., Ross, D., Trush, M. A., Zweier, J. L., & Li, Y. (2006). Nrf2 controls bone marrow stromal cell susceptibility to oxidative and electrophilic stress. *Free Radical Biology & Medicine, 41*, 132–143. doi:10.1016/j.freeradbiomed.2006.03.020.

14. Spitz, D. R., & Oberley L. W. (1989). An assay for superoxide dismutase activity in mammalian tissue homogenates. *Analytical Biochemistry, 179*, 8–18. doi:10.1016/0003-2697(89)90192-9.

15. Aebi, H. (1984). Catalase in vitro. *Methods in Enzymology*, *105*, 121–127. doi:10.1016/S0076-6879(84)05016-3.

16. Flohé L, & Günzler W. A. (1984). Assays of glutathione peroxidase. *Methods in Enzymology*, *105*, 114–121. doi:10.1016/S0076–6879(84)05015-1.

17. Habig, W. H., Pabst, M. J., & Jakoby, W. B. (1974). Glutathione S-transferases: The first enzymatic step in mercapturic acid formation. *The Journal of Biological Chemistry*, *249*, 7130–7139.

18. Naughton, P., Foresti, R., Bains, S. K., Hoque, M., Green, C. J., & Motterlini, R. (2002). Induction of heme oxygenase 1 by nitrosative stress. A role for nitroxyl anion. *The Journal of Biological Chemistry, 277*, 40666–40674. doi:10.1074/jbc.M203863200.

19. Zhu, H., Zhang, L., Trush, M. A., & Li, Y. (2007). Upregulation of endogenous glutathione system by 3*H*-1,2-dithiole-3-thione in pancreatic RINm5F beta-cells as a novel strategy for protecting against oxidative beta-cell injury. *Free Radical Research, 41*, 242–250. doi:10.1080/10715760601009586.

20. Jia, Z., Zhu, H., Misra, H. P., & Li, Y. (2008). Potent induction of total cellular GSH and NQO1 as well as mitochondrial GSH by 3*H*-1,2-dithiole-3-thione in SH-SY5Y neuroblastoma cells and primary human neurons: Protection against neurocytotoxicity elicited by dopamine, 6-hydroxydopamine, 4-hydroxy-2-nonenal, or hydrogen peroxide. *Brain Research, 1197*, 159–169. doi:10.1016/j.brainres.2007.12.044.

21. Halford, W. P., Falco, V. C., Gebhardt, B. M., & Carr, D. J. (1999). The inherent quantitative capacity of the reverse transcription-polymerase chain reaction. *Analytical Biochemistry, 266*, 181–191. doi:10.1006/abio.1998.2913.

22. Hayes, J. D., Flanagan, J. U., & Jowsey, I. R. (2005). Glutathione transferases. *Annual Review of Pharmacology and Toxicology, 45*, 51–88. doi:10.1146/annurev.pharmtox.45.120403.095857.

23. Abraham, N. G., & Kappas, A. (2005). Heme oxygenase and the cardiovascular-renal system. *Free Radical Biology & Medicine, 39*, 1–25. doi:10.1016/j.freeradbiomed.2005.03.010.

24. Ryter, S. W., Alam, J., & Choi, A. M. (2006). Heme oxygenase-1/carbon monoxide: From basic science to therapeutic applications.*Physiological Research, 86*, 583–650. doi:10.1152/physrev.00011.2005.

25. Szabó C, Ischiropoulos, H., & Radi, R. (2007) Peroxynitrite: Biochemistry, pathophysiology and development of therapeutics. *Nature Reviews. Drug Discovery, 6*, 662–680. doi:10.1038/nrd2222.

26. Lucas, D. T., & Szweda, L. I. (1998). Cardiac reperfusion injury: Aging, lipid peroxidation, and mitochondrial dysfunction. *Proceedings of the National Academy of Sciences of the United States of America, 95*, 510–514. doi:10.1073/pnas.95.2.510.

27. Shinmura, K., Bolli, R., Liu, S. Q., Tang, X. L., Kodani, E., Xuan, Y. T., Srivastava, S., & Bhatnagar A (2002). Aldose reductase is an obligatory mediator of the late phase of ischemic preconditioning. *Circulation Research, 91*, 240–246. doi:10.1161/01.RES.0000029970.97247.57.

28. Cho, H. Y., Reddy, S. P., Debiase, A., Yamamoto, M., & Kleeberger, S. R. (2005). Gene expression profiling of Nrf2-mediated protection against oxidative injury. *Free Radical Biology & Medicine, 38*, 325–343. doi:10.1016/j.freeradbiomed.2004.10.013.

29. Kwak, M. K., Wakabayashi, N., Itoh, K., Motohashi, H., Yamamoto, M., & Kensler, T. W. (2003). Modulation of gene expression by cancer chemopreventive dithiolethiones through the Keap1-Nrf2 pathway: Identification of novel gene clusters for cell survival. *The Journal of Biological Chemistry, 278*, 8135–8145. doi:10.1074/jbc.M211898200.

30. Zhu, H., Itoh, K., Yamamoto, M., Zweier, J. L., & Li, Y. (2005). Role of Nrf2 signaling in regulation of antioxidants, phase 2 enzymes in cardiac fibroblasts: Protection against reactive oxygen and nitrogen species-induced cell injury. *FEBS Letters, 579*, 3029–3036. doi:10.1016/j.febslet.2005.04.058.

31. Anderson, M. E. (1998). Glutathione: An overview of biosynthesis and modulation. *Chemico-Biological Interactions, 111–112*, 1–14. doi:10.1016/S0009-2797(97)00146-4.

32. Banning, A., Deubel, S., Kluth, D., Zhou, Z., & Brigelius-Flohe, R. (2005). The GI-GPx gene is a target for Nrf2. *Molecular and Cellular Biology, 25*, 4914–4923. doi:10.1128/MCB.25.12.4914-4923.2005.

33. Li, Y., Lafuente, A., & Trush, M. A. (1994). Characterization of quinone reductase, glutathione and glutathione S-transferase in human myeloid cell lines: Induction by 1,2-dithiole-3-thione and effects on hydroquinone-induced cytotoxicity. *Life Sciences, 54*, 901–916. doi:10.1016/0024-3205(94)00626-1.

34. Ross, D. (2004). Quinone reductases multitasking in the metabolic world. *Drug Metabolism Reviews, 36*, 639–654. doi:10.1081/DMR-200033465.

35. Siegel, D., Gustafson D. L, Dehn, D. L., Han, J. Y., Boonchoong, P., Berliner, L. J., & Ross, D. (2004). NAD(P)H: Quinone oxidoreductase 1: Role as a superoxide scavenger. *Molecular Pharmacology, 65*, 1238–1247. doi:10.1124/mol.65.5.1238.

36. Zhu, H., Jia, Z., Mahaney, J. E., Ross, D., Misra, H. P., Trush, M. A., & Li, Y. (2007). The highly expressed and inducible endogenous NAD(P)H: Quinone oxidoreductase 1 in cardiovascular cells acts as a potential superoxide scavenger. *Cardiovascular Toxicology, 7*, 202–211. doi:10.1007/s12012-007-9001-z.

37. Asher, G., Lotem, J., Kama, R., Sachs, L., & Shaul, Y. (2002). NQO1 stabilizes p53 through a distinct pathway. *Proceedings of the National Academy of Sciences of the United States of America, 99*, 3099–3104. doi:10.1073/pnas.052706799.

38. Juan, S. H., Lee, T. S., Tseng, K. W., Liou, J. Y., Shyue, S. K., Wu, K. K., & Chau, L. Y. (2001). Adenovirus-mediated heme oxygenase-1 gene transfer inhibits the development of atherosclerosis in apolipoprotein E-deficient mice. *Circulation, 104*, 1519–1525. doi:10.1161/hc3801.095663.

39. Liu, X., Simpson, J. A., Brunt, K. R., Ward, C. A., Hall, S. R., Kinobe, R. T., Barrette, V., Tse, M. Y., Pang, S. C., Pachori, A. S., Dzau, V. J., Ogunyankin, K. O., & Melo, L. G. (2007). Preemptive heme oxygenase-1 gene delivery reveals reduced mortality and preservation of left ventricular function 1 yr after acute myocardial infarction. *The American Journal of Physiology, 293*, H48–H59.

40. Sies, H., Sharov, V. S., Klotz, L. O., & Briviba, K. (1997). Glutathione peroxidase protects against peroxynitrite-mediated oxidations: A new function for selenoproteins as peroxynitrite reductase. *The Journal of Biological Chemistry, 272*, 27812–27817. doi:10.1074/jbc.272.44.27812.

41. Xie, C., Lovell, M. A., Xiong, S., Kindy, M. S., Guo J.-T., Xie, J., Amaranth, V., Montine, T. J., & Markesbery, W. R. (2001). Expression of glutathione-S-transferase isozyme in the SY5Y

neuroblastoma cell line increases resistance to oxidative stress. *Free Radical Biology & Medicine, 31*, 73–81. doi:10.1016/S0891-5849(01)00553-6.

42. Yang, Y., Cheng J.-Z., Singhal, S. S., Saini, M., Pandya, U., Awasthi, S., & Awasthi, Y. C. (2001). Role of glutathione S-transferases in protection against lipid peroxidation. *The Journal of Biological Chemistry, 276*, 19220–19230. doi:10.1074/jbc.M100551200.

43. Sayre, L. M., Lin, D., Yuan, Q., Zhu, X., & Tang, X. (2006). Protein adducts generated from products of lipid oxidation: Focus on HNE and one.*Drug Metabolism Reviews, 38*, 651–675. doi:10.1080/03602530600959508.

44. Cao, Z., Hardej, D., Trombetta, L. D., & Li, Y. (2003). The role of chemically induced glutathione and glutathione S-transferase in protecting against 4-hydroxy-2-nonenal-mediated cytotoxicity in vascular smooth muscle cells. *Cardiovascular Toxicology, 3*, 165–177. doi:10.1385/CT:3,2:165.

45. Li, Y., Cao, Z., Zhu, H., & Trush, M. A. (2005). Differential roles of 3*H*-1,2-dithiole-3-thione-induced glutathione, glutathione S-transferase and aldose reductase in protecting against 4-hydroxy-2-nonenal toxicity in cultured cardiomyocytes. *Archives of Biochemistry and Biophysics, 439*, 80–90. doi:10.1016/j.abb.2005.05.008.